THE UNIVERSITY *of* EDINBURGH

Edinburgh Research Explorer

Effects of FDMA/TDMA Orthogonality on the Gaussian Pulse Train MIMO Ambiguity Function

Citation for published version:
Shtarkalev, B & Mulgrew, B 2015, 'Effects of FDMA/TDMA Orthogonality on the Gaussian Pulse Train MIMO Ambiguity Function' IEEE Signal Processing Letters, vol. 22, no. 2, pp. 153-157. DOI: 10.1109/LSP.2014.2351256

Digital Object Identifier (DOI):
10.1109/LSP.2014.2351256

Published In:
IEEE Signal Processing Letters

Effects of FDMA/TDMA Orthogonality on the Gaussian Pulse Train MIMO Ambiguity Function

Bogomil Shtarkalev and Bernard Mulgrew, *Fellow, IEEE*

Abstract

As multiple-input multiple-output (MIMO) radar gains popularity, more efficient and better-performing detection algorithms are developed to exploit the benefits of having more transmitters and receivers. Many of these algorithms are based on the assumption that the multiple waveforms used for target scanning are orthogonal to each other in fast time. It has been shown that this assumption can limit the practical detector performance due to the reduction of the area that is clear of sidelobes in the MIMO radar ambiguity function. In this work it is shown that using the same waveform with a different carrier frequency and/or delay across different transmitters ensures relative waveform orthogonality while alleviating the negative effects on the ambiguity function. This is demonstrated in a practical scenario where the probing waveforms consist of Gaussian pulse trains (GPTs) separated in frequency. An approximate theoretical model of the ambiguity is proposed and it is shown that the effects of cross-ambiguity in the MIMO system are negligible compared to the waveform autoambiguities.

Index Terms

Ambiguity function, MIMO radar, Gaussian pulse waveforms, Gaussian approximation

I. Introduction

Multiple-input multiple-output (MIMO) radar with widely-separated antennas is a widespread research area that has gained an increasing popularity over the past decade. The advantages of using multiple transmitters and receivers are numerous: higher accuracy of target localisation, higher detection rate, increased spatial and angular diversity, increased resolution [1]–[6]. Many algorithms have been proposed in the past that in theory provide very promising performance gains for larger MIMO radar networks [1]–[6]. It has been shown in theory [7] and practice [8] that these algorithms often ignore the limiting factor of the MIMO ambiguity function. These effects can degrade the performance of a radar setup that uses a number of orthogonal waveforms in fast time. In a MIMO scenario, the maximum area in the ambiguity function that can be cleared of sidelobes gets proportionally smaller as the number of such waveforms increases [7], [8]. That lowers the effective signal-to-interference and noise ratio (SINR) which in turn degrades the overall detection performance.

In this work it will be shown that in a widely-spaced MIMO radar system the limiting factors of the ambiguity function can be alleviated if the transmitted waveforms are separated in time and/or frequency. The concept is identical to frequency-division multiple access (FDMA) and time-division multiple access (TDMA) in wireless communication [9]. If the radar pulses are band-limited to sufficiently separated bands, the cross-ambiguity contributions to the total MIMO ambiguity are negligible. The effects have been demonstrated for a Gaussian pulse train (GPT) waveform with no delays and small Doppler shifts. An approximation to the ratio of cross-to-auto-ambiguity has been derived and simulated for the case investigated in this work. The benefits of the proposed methods come at the price of an increased bandwidth or delay in the MIMO radar system. While the derivations are performed for GPTs for convenience, guidelines for extending the approach to a wider variety of waveforms are discussed.

The rest of this paper is organised as follows. Section II provides a description of the ambiguity function and introduces the ambiguity of an infinite GPT. Section III derives the autoambiguity of a finite GPT, and Section IV derives the cross-ambiguity between two FDMA-orthogonal GPTs. In Section V the volume ratio of cross-to-autoambiguity is introduced as a metric for interference between waveforms. A Gaussian approximation to the Fejér kernel is proposed in order to derive a theoretical expression for the volume ratio of the GPT. Section VI demonstrates the viability of the proposed approximation and shows that the cross-ambiguity terms in the MIMO ambiguity function can be effectively ignored.

II. Background

Woodward's ambiguity function of a continuous narrowband signal $u(t)$ is defined as [10], [11]

$$\alpha(t,f) = \int_{-\infty}^{\infty} u\left(\tau - \frac{1}{2}t\right) u^*\left(\tau + \frac{1}{2}t\right) e^{-j2\pi f\tau} d\tau \tag{1}$$

Manuscript received July 02, 2014; revised August 13, 2014; accepted August 14, 2014. The associate editor coordinating the review of this manuscript and approving it for publication was Prof. Qian He. This work was supported by the Institute for Digital Communications at the University of Edinburgh, Selex ES and EPSRC(EP/J015180/1).

The authors are with the Institute for Digital Communications, School of Engineering, The University of Edinburgh, Edinburgh, EH9 3JL, U.K. (e-mail: B.Shtarkalev@ed.ac.uk; B.Mulgrew@ed.ac.uk)

where the subscript $*$ denotes the complex conjugate. At f=0 the integral (1) reduces to the standard time-domain autocorrelation function of $u(t)$. A waveform with a well-known ambiguity function is the Gaussian pulse (GP)

$$u_g(t) = \left(\frac{2a}{\pi}\right)^{\frac{1}{4}} \exp\left\{-at^2\right\} \tag{2}$$

where the parameter a is related to the standard deviation σ and thus the width of the GP.

$$a = \frac{1}{2\sigma^2} \tag{3}$$

The ambiguity of the GP is a two-dimensional Gaussian function extending in time and frequency [10], [11]

$$\alpha_g(t,f) = \exp\left(-\frac{1}{2}at^2\right)\exp\left(-\frac{\pi^2 f^2}{2a}\right) \tag{4}$$

A radar waveform consists of multiple pulses. To obtain the ambiguity function of a GPT, the following property can be used: if two waveforms are convolved in time, their ambiguity functions are convolved in time [10]. An infinite GPT is the convolution of a GP and a train of Dirac delta functions

$$u_\delta(t) = \sum_{k=-\infty}^{\infty} \delta(t - kR) \tag{5}$$

spaced at a distance R. The ambiguity function of (5) takes the well-known "bed of nails" form [10, pp.6-8]

$$\alpha_\delta(t,f) = \sum_n \sum_m \delta(t - nR)\delta(f - m/R) \tag{6}$$

The ambiguity function of an infinite GPT will be the convolution of (4) and (6) along the time axis. The spacing R is equal to the length of each GP, which this work defines as 6 times its standard deviation σ. Plugging this into (3) results in

$$a = \frac{18}{R^2} \tag{7}$$

The ambiguity function of the infinite GPT consists of shifted copies of (4) in time at t=nR sampled along frequency at f=mR^{-1}. The waveform is reminiscent of a "bed of razors" which are infinitely long and infinitesimally wide.

III. Finite Gaussian Pulse Train Ambiguity

In a real scenario a radar transmits a finite number of pulses. Consider a GPT of K consecutive GPs. It is the convolution of (2) and a train of K equally-spaced Dirac delta functions.

$$u_{K\delta}(t) = \frac{1}{\sqrt{K}} \sum_{k=0}^{K-1} \delta(t - kR) \tag{8}$$

The normalising constant in (8) ensures that the energy in the waveform remains unity. The ambiguity function of (8) can be calculated through direct evaluation of the integral in (1). The result is a symmetric sum of Dirac delta functions along the time axis and a sum of exponentials along frequency

$$\begin{aligned}\alpha_{K\delta}(t,f) =& \frac{1}{K} \sum_{p=-K+1}^{0} \delta(t - pR) \sum_{k=0}^{K+p-1} e^{-j2\pi fkR} \\ &+ \frac{1}{K} \sum_{p=1}^{K-1} \delta(t - pR) \sum_{k=p}^{K-1} e^{-j2\pi fkR}\end{aligned} \tag{9}$$

To facilitate the analysis, define the following expression

$$D_n(x) = \frac{\sin(\pi n x)}{\sin(\pi x)} \tag{10}$$

which is a special case of the Dirichlet kernel function. The formula for a geometric series of exponentials is

$$\sum_{k=0}^{K-1} e^{-j2\pi fkR} = D_K(fR) e^{-j\pi f(K-1)R} \tag{11}$$

The volume of the ambiguity function in a given area is used as a measure of waveform orthogonality in MIMO radar detection [7]. Thus it can limit the performance of MIMO radar. The normalised ambiguity of the finite GPT is obtained after convolving (4) and (9) in time and through using (11)

$$|\alpha_{Kg}(t,f)| = \frac{1}{K} \sum_{k=-K+1}^{K-1} \alpha_g(t - kR, f) |D_{K-|k|}(fR)| \tag{12}$$

As the number of pulses K approaches infinity, the Dirichlet kernel (10) becomes an arbitrarily close approximation to an infinite Dirac delta train in frequency, and the ambiguity function takes the form described at the end of Section II. The volume of the ambiguity function $\alpha(t,f)$ in a region A is

$$V(A) = \iint_A |\alpha(t,f)|^2 df dt \tag{13}$$

Due to the shape of $\alpha_g(t,f)$ and since the distance R is equal to 6σ, the cross-terms when squaring the right hand side of (12) involve Gaussian tails and can be ignored. Thus the following approximation can be made

$$|\alpha_{Kg}(t,f)|^2 \approx \frac{1}{K^2}\sum_{k=-K+1}^{K-1} \alpha_g(t-kR,f)^2 F_{K-|k|}(fR) \tag{14}$$

$F_n(x)$ is the Fejér kernel defined here as (10) squared.

$$F_n(x) = \frac{\sin(\pi n x)^2}{\sin(\pi x)^2} \tag{15}$$

Essentially (14) ignores the tail contributions from neighbouring GPs to the peaks centred around $t{=}kR$. The volume of the ambiguity of the GPT in an area A around the origin is

$$V^{\alpha}_{Kg}(A){=}\frac{1}{K^2}\sum_k \iint_A \alpha_g(t-kR,f)^2 F_{K-|k|}(fR) df dt \tag{16}$$

The limits of the sum in (16) have been omitted. Usually the aim is to make the volume as close to the ideal case $V(A){=}\delta(t)\delta(f)$ as possible, and thus small regions A around the origin are considered. The contribution to such a region will come from no more than the set $k \in \{-1,0,1\}$ in (16).

IV. Waveform Cross-Ambiguity in a Multiple Access MIMO Scenario

The waveforms in a MIMO radar scenario are usually considered orthogonal and ideally separable [1]–[5]. In reality this is not achievable; however, there are transmission schemes similar to FDMA and TDMA which result in low cross-correlation waveforms. Thus the waveforms are "orthogonal" in frequency or time. Consider the GP (2) and an interferer separated in frequency by an offset $f_\triangle$ and in time by $t_\triangle$

$$u_i(t) = \left(\frac{2a}{\pi}\right)^{\frac{1}{4}} e^{-a(t-t_\triangle)^2} e^{-j2\pi f_\triangle t} \tag{17}$$

The duration and bandwidth of (2) and (17) are the same. The cross-ambiguity between the two waveforms is defined as

$$\chi_g(t,f) = \int_{-\infty}^{\infty} u_g\left(\tau - \frac{1}{2}t\right) u_i^*\left(\tau + \frac{1}{2}t\right) e^{-j2\pi f \tau} d\tau \tag{18}$$

One can either solve the integral (18) or use the fact that the pulse (17) is (2) convolved in time with $\delta(t-t_\triangle)$ and in frequency with $\delta(f-f_\triangle)$ to obtain the cross-ambiguity

$$\chi_g(t,f){=}e^{-j\phi}\exp\left(-\frac{a(t{-}t_\triangle)^2}{2}\right)\exp\left(-\frac{\pi^2(f{-}f_\triangle)^2}{2a}\right) \tag{19}$$

where ϕ is a time-frequency phase term. As expected, (19) is simply a shifted version of (4) in time and frequency.

$$|\chi_g(t,f)| = |\alpha_g(t-t_\triangle, f-f_\triangle)| \tag{20}$$

For simplicity it is assumed that each GPT contains K pulses. Following the approach in Section III, the normalised cross-ambiguity of two GPTs offset in time and frequency is

$$|\chi_{Kg}(t,f)|{=}\frac{1}{K}\sum_{k=-K+1}^{K-1}|\chi_g(t{-}kR,f) D_{K-|k|}((f{-}f_\triangle)R)| \tag{21}$$

The approximation to the squared magnitude is once again

$$|\chi_{Kg}(t,f)|^2{\approx}\frac{1}{K^2}\sum_{k=-K+1}^{K-1}|\chi_g(t{-}kR,f)|^2 F_{K-|k|}((f{-}f_\triangle)R) \tag{22}$$

The formula for the volume of (22) is the same as (16) with the area A centred around $(t_\triangle, f_\triangle)$ instead of $(0,0)$. The Fejér kernel is $1/R$-periodic. Thus most of the volume of (22) is contained around the points $(kR{-}t_\triangle, n/R{-}f_\triangle)$ where n is an integer and k is within the limits given in the sums above.

V. Ambiguity Volume Ration in a Multiple Access MIMO Scenario

A. Volume Ratio in an FDMA Scenario

The aim of orthogonal waveform design is to reduce the volume of the cross-ambiguity (22) around the origin. The worst-case scenario is when the waveforms are offset by a multiple of R in time and $1/R$ in frequency. The bandwidth of the GP (2) can be obtained through its Fourier transform

$$U_g(f) = \left(\frac{2a}{\pi}\right)^{\frac{1}{4}} \exp\left\{-\frac{f^2\pi^2R^2}{18}\right\} \tag{23}$$

If the 6σ width rule is also applied to (23), the double-sided width of the spectrum of a GP is

$$B_W = \frac{18}{\pi R} \approx \frac{6}{R} \tag{24}$$

This is 6 times the rule of thumb $B_W{\approx}1/R$ but renders the spectrum of the GP practically band-limited. Under this assumption, the width of the spectrum of a GPT will not exceed (24). In an FDMA system the channel separation will usually be at least equal to the channel width. Therefore one can assume $f_\Delta{\geq}B_W$. Also assume that the Doppler shifts of the waveforms are small relative to their bandwidths to eliminate interchannel interference. The 6σ width of the ambiguity $|\alpha_g(f,t)|^2$ in frequency is also B_W. The worst-case scenario is $f_\Delta{=}6/R$, where also the Fejér kernel peaks.

An FDMA system is considered here, but the results can be extended to TDMA. Thus it is assumed that no time delays between waveforms occur ($t_\Delta{=}0$). In a MIMO system with M transmitters and N receivers the total ambiguity is defined as the sum of all channel cross- and auto-ambiguities [7], [12]

$$|\chi_{MN}(t,f)|^2 = \sum_{m=1}^{M}\sum_{n=1}^{N}|\chi_{mn}(t,f)|^2 \tag{25}$$

The aim to reduce cross-ambiguities means that (25) can reduce to the sum of autoambiguities. Thus in this work the volume ratio between the cross- and auto-ambiguity of waveforms is introduced as a measure of self-interference in MIMO radar. The volume ratio is investigated in a small rectangular region A around the origin where only the $k{=}0$ terms contribute significantly. The volume ratio reduces to

$$V_r = \frac{\int \exp\left(-\frac{\pi^2(f-f_\Delta)^2}{a}\right) F_K((f-f_\Delta)R)df}{\int \exp\left(-\frac{\pi^2 f^2}{a}\right) F_K(fR)df} \tag{26}$$

since the integral with respect to time is the same in the numerator and denominator. The integration of multiplications of Gaussian and sinusoid functions in (26) can only be done numerically. A theoretical result could be obtained if the Fejér kernel is approximated by a Gaussian function.

B. Fejér Kernel Gaussian Approximation

The Fejér kernel in (15) is a $1/R$-periodic non-negative function. Consider one period of (15) centred around the origin. It takes the form of a rapidly decaying oscillation where the first zero-crossing is at $f{=}\pm1/n$. The mainlobe of the Fejér kernel can thus be approximated by a Gaussian with a $6\sigma_f$ width of $2/n$. Consider the Fejér kernel from (26). The signal is scaled by R and shifted by f_Δ. The periodicity of the kernel will be represented in the approximation as an infinite sum of Gaussian functions. The approximation is therefore

$$\tilde{F}_K((f-f_\Delta)R)=\sum_n K^2\exp\left(-\frac{9}{2}K^2\left(f-f_\Delta-\frac{n}{R}\right)^2 R^2\right) \tag{27}$$

Plugging (27) in (26), the expression inside the integral is a sum of products of two Gaussian functions. Each of these products is Gaussian with mean $\mu_c(n)$ and variance σ_c^2 [13]

$$\mu_c(n) = f_\Delta + \mu_p(n) \tag{28}$$

$$\mu_p(n) = 9K^2R\sigma_c^2 n \tag{29}$$

$$\sigma_c^2 = \frac{9}{R^2((3K)^2+\pi^2)} \tag{30}$$

where $\mu_p(n)$ are the means in the denominator of (26). Consider a rectangular symmetric region around the origin $\{|t|\leq t_b, |f|\leq f_b\}$. For $t_b<R/2$ only the ambiguity around $k=0$ is considered. The volume ratio approximation is

$$\tilde{V}_r(f_b)=\frac{\sum\limits_n \int\limits_{-f_b}^{f_b} \exp\left(-\frac{(f-\mu_c(n))^2}{2\sigma_c^2}\right)\exp\left(-\frac{\pi^2\mu_p^2(n)}{a}\right)df}{\sum\limits_n \int\limits_{-f_b}^{f_b} \exp\left(-\frac{(f-\mu_p(n))^2}{2\sigma_c^2}\right)\exp\left(-\frac{\pi^2\mu_p^2(n)}{a}\right)df}$$

$$=\frac{\sum\limits_n \exp\left(-\frac{\pi^2\mu_p^2(n)}{a}\right)\left[\operatorname{erf}\left(\frac{f_b+\mu_c(n)}{\sigma_c}\right)-\operatorname{erf}\left(-\frac{f_b-\mu_c(n)}{\sigma_c}\right)\right]}{\sum\limits_n \exp\left(-\frac{\pi^2\mu_p^2(n)}{a}\right)\left[\operatorname{erf}\left(\frac{f_b+\mu_p(n)}{\sigma_c}\right)-\operatorname{erf}\left(-\frac{f_b-\mu_p(n)}{\sigma_c}\right)\right]} \tag{31}$$

where each contributing factor along the frequency axis is scaled accordingly. The sum over the integer n in (31) represents the contributions of the different Gaussian shapes along the frequency axis to the volume in the area A. As usually this area of interest is small, only a few of the contributors around $n=0$ are enough to represent the whole sum.

VI. Simulations

A small MIMO radar system with two FDMA-orthogonal GPT waveforms has been simulated. The length of each individual GP is R=2ms, and the bandwidth is B_W=3kHz. The worst-case scenario of f_Δ=3kHz is investigated. Fig. 1 shows an example of a GPT ambiguity (12) at t=0 alongside its approximation (14) with the Gaussian model (27) for the Fejér kernel. Due to the

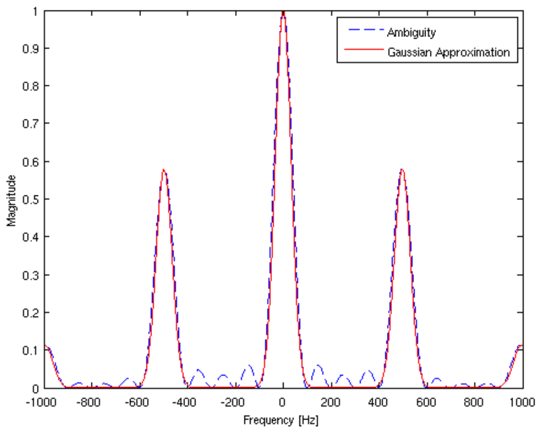

Fig. 1. Autoambiguity of a 5-pulse waveform at t=0 with Gaussian approximation to the Fejér kernel

nature of the fitting described in Section V-B, the model predicts the behaviour of the ambiguity well at the mainlobes of the Fejér kernel. All sidelobes outside the mainlobes, however, are ignored by the model. Thus it is expected for the approximate model of the volume ratio (31) to also best match the theoretical values around the peaks of the Fejér kernel. This can be seen in the results in Fig. 2 where the theoretical and actual volume ratios are shown for GPTs of K=4 and K=40 pulses. The simulated volume ratio (26) is calculated through numeric integration in a rectangular area A bounded by t_b=1ms. The bound in frequency f_b is varied along the x-axis in Fig. 2. As predicted, the theoretical model closely approximates the volume ratio (26) around the points n/R where the Fejér kernel peaks. Between the mainlobes the theoretical model underestimates the volume ratio since it ignores the sidelobes. The general behaviour of the volume ratio is relatively well predicted through the proposed estimator (31) which does not involve numeric integration. The results in Fig. 2 show that the volume of the cross-ambiguity function in a rectangular area centred at the origin of the range-Doppler space is at least 40dB lower than the volume of the autoambiguity in the same area. Therefore in the system (25) with M transmitters and N receivers, the total ambiguity can be approximated as strictly the sum of the autoambiguities

$$|\chi_{MN}(t,f)|^2 \approx \sum_{m=1}^{M} |\chi_{mm}(t,f)|^2 \tag{32}$$

This reflects the waveform orthogonality achieved through FDMA. The tradeoff is the increased bandwidth of the system used by the additional channels. A MIMO system of M orthogonal waveforms requires a bandwidth of MB_W. This limits the FDMA waveform design to small radar networks.

The analysis in this work is performed on GPTs for convenience. Note that the approximations (14) and (22) hold for any pulse with ambiguity $\alpha(t,f)$ that can be neglected outside of a region R along the time axis. However, one must ensure the

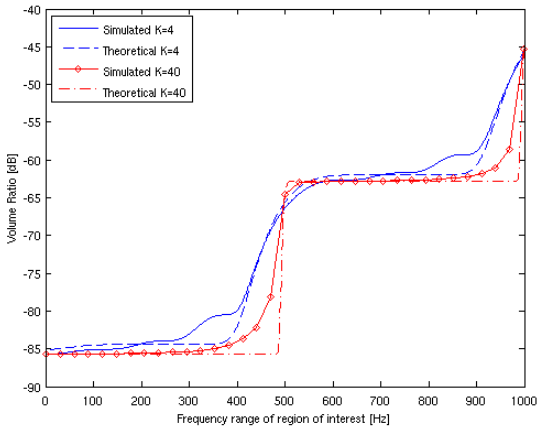

Fig. 2. Volume ratio of cross-ambiguity to autoambiguity in a rectangular region A for FDMA-orthogonal radar waveforms

spacing between pulses in (8) is also greater than R. If the pulses forming a waveform meet these conditions, the autoambiguity at the origin and around f_Δ as well as the Fejér kernel weights at those points can be used as a rough estimate of the behaviour of the waveform volume ratio. Note that the Gaussian approximation to the Fejér kernel (27) is independent of the shape of the transmitted waveforms.

VII. Conclusion

In this work the volume of the ambiguity and cross-ambiguity function of GPT waveforms separated in frequency has been analysed. The waveforms could be but are not limited to pilots in an FDMA MIMO radar scenario where through increase of bandwidth, interference between different transmitters is minimised. A theoretical model for the volume ratio of the cross- and auto-ambiguity functions is proposed that is inexpensive in terms of processing power and can predict the amount of interference between waveforms in the Doppler-range ambiguity space. Through this model it is demonstrated that if channels in an FDMA MIMO radar scenario are sufficiently separated in frequency, virtually no interference between transmitters occurs in the MIMO ambiguity function.

Acknowledgment

The authors would like to thank the associate editor Prof. Qian He and the anonymous reviewers for their comments that helped improve the final version of this manuscript.

REFERENCES

[1] E. Fishler, A. Haimovich, R. Blum, D. Chizhik, L. Cimini, and R. Valenzuela, "MIMO radar: an idea whose time has come," in *Radar Conference, 2004. Proceedings of the IEEE*, pp. 71 – 78, april 2004.

[2] A. Haimovich, R. Blum, and L. Cimini, "MIMO radar with widely separated antennas," *Signal Processing Magazine, IEEE*, vol. 25, no. 1, pp. 116 –129, 2008.

[3] W. Melvin, R. Hancock, M. Rangaswamy, and J. Parker, "Adaptive distributed radar," in *Radar Conference - Surveillance for a Safer World, 2009. RADAR. International*, pp. 1–6, Oct 2009.

[4] D. Bruyere and N. Goodman, "Adaptive detection and diversity order in multistatic radar," *Aerospace and Electronic Systems, IEEE Transactions on*, vol. 44, pp. 1615 –1623, oct. 2008.

[5] L. Kong, M. Yang, and B. Zhao, "Adaptive detection for shared-spectrum multistatic radar in Gaussian clutter," in *Radar Conference (RADAR), 2012 IEEE*, pp. 0309 –0313, may 2012.

[6] B. Shtarkalev and B. Mulgrew, "Multistatic single data set target detection in unknown coloured Gaussian interference," in *Radar Conference (RADAR), 2013 IEEE*, pp. 1–5, 2013.

[7] Y. Abramovich and G. J. Frazer, "Bounds on the volume and height distributions for the MIMO radar ambiguity function," *Signal Processing Letters, IEEE*, vol. 15, pp. 505–508, 2008.

[8] G. Frazer, Y. Abramovich, and B. Johnson, "MIMO radar limitations in clutter," in *Radar Conference, 2009 IEEE*, pp. 1–5, 2009.

[9] I. Glover and P. Grant, *Digital Communications*. Pearson Prentice Hall, 3rd ed., 2010.

[10] P. M. Woodward, "Radar ambiguity analysis," tech. rep., DTIC Document, 1967.

[11] D. Swick, "A review of narrowband ambiguity functions," tech. rep., DTIC Document, 1970.

[12] G. San Antonio, D. Fuhrmann, and F. Robey, "MIMO radar ambiguity functions," *Selected Topics in Signal Processing, IEEE Journal of*, vol. 1, no. 1, pp. 167–177, 2007.

[13] P. A. Bromiley, "Products and convolutions of Gaussian distributions," Internal Report Tina Memo No. 2003-003, Imaging Science and Biomedical Engineering Division Medical School, University of Manchester, Nov 2003.